The Journal of Neuroscience, December, 15, 2000, *20*(24):9059–9070

Origin Sites of Calcium Release and Calcium Oscillations in Frog Sympathetic Neurons

Stefan I. McDonough, Zoltán Cseresnyés, and Martin F. Schneider

Department of Biochemistry and Molecular Biology, University of Maryland Medical School, Baltimore, Maryland 21201

In many neurons, Ca^{2+} signaling depends on efflux of Ca^{2+} from intracellular stores into the cytoplasm via caffeine-sensitive ryanodine receptors (RyRs) of the endoplasmic reticulum. We have used high-speed confocal microscopy to image depolarization- and caffeine-evoked increases in cytoplasmic Ca^{2+} levels in individual cultured frog sympathetic neurons. Although caffeine-evoked Ca^{2+} wave fronts propagated throughout the cell, in most cells the initial Ca^{2+} release was from one or more discrete sites that were several micrometers wide and located at the cell edge, even in Ca^{2+}-free external solution. During cell-wide cytoplasmic [Ca^{2+}] oscillations triggered by continual caffeine application, the initial Ca^{2+} release that began each Ca^{2+} peak was from the same subcellular site or sites. The Ca^{2+} wave fronts propagated with constant amplitude; the spread was mostly via calcium-induced calcium release. Propagation was faster around the cell periphery than radially inward. Local Ca^{2+} levels within the cell body could increase or decrease independently of neighboring regions, suggesting independent action of spatially separate Ca^{2+} stores. Confocal imaging of fluorescent analogs of ryanodine and thapsigargin, and of MitoTracker, showed potential structural correlates to the patterns of Ca^{2+} release and propagation. High densities of RyRs were found in a ring around the cell periphery, mitochondria in a broader ring just inside the RyRs, and sarco-endoplasmic reticulum Ca^{2+} ATPase pumps in hot spots at the cell edge. Discrete sites at the cell edge primed to release Ca^{2+} from intracellular stores might preferentially convert Ca^{2+} influx through a local area of plasma membrane into a cell-wide Ca^{2+} increase.

Key words: ryanodine receptor; sympathetic neuron; caffeine; confocal microscopy; calcium; calcium wave; calcium oscillations; calcium-induced calcium release; subsurface cistern; fluo-4

Cytoplasmic Ca^{2+} levels in neurons govern many signaling processes, including neurotransmitter secretion, regulation of membrane excitability, and induction of gene expression (Kennedy, 1989; Clapham, 1995; Ghosh and Greenberg, 1995). Cytoplasmic Ca^{2+} concentrations are increased by influx of extracellular Ca^{2+} through plasma membrane Ca^{2+} channels and by release of Ca^{2+} from within intracellular organelles, especially the endoplasmic reticulum (ER), that serve as Ca^{2+} stores (Berridge, 1998). Although the ER may be a continuous membrane system throughout the neuron (Berridge, 1998), different parts of the ER may act separately for purposes of Ca^{2+} signaling (Golovina and Blaustein, 1997; Meldolesi and Pozzan, 1998). Two prominent pathways for release of Ca^{2+} from within the ER into the cytoplasm are via ryanodine receptors (RyRs) or inositol 1,4,5-trisphosphate receptors ($InsP_3Rs$) located on the ER membrane. Both molecules are Ca^{2+} channels that are themselves gated by cytoplasmic Ca^{2+}; RyRs are also opened pharmacologically by millimolar concentrations of caffeine (Rousseau et al., 1988; McPherson et al., 1991). Local Ca^{2+} release can induce Ca^{2+} release from neighboring sites, amplifying the initial release into Ca^{2+} wave fronts.

Oscillations of cytoplasmic Ca^{2+} levels are a striking form of signaling in which RyRs or $InsP_3Rs$ govern repetitive release from intracellular Ca^{2+} stores in response to a constant external stimulus. Such oscillations occur with distinct frequencies and shapes and have been observed in many kinds of excitable and nonexcitable cells (Tsien and Tsien, 1990; Fewtrell, 1993). Oscillations evoke secretion in hepatocytes, pancreatic acinar cells, and gonadotrophs (Tepikin and Petersen, 1992; Hille et al., 1994). The precise oscillation frequency has been shown to control specific patterns of gene expression (Dolmetsch et al., 1998; Li et al., 1998), the activation of Ca^{2+}-sensitive enzymes (De Koninck and Schulman, 1998), and the speed and direction of neuronal migration (Gu and Spitzer, 1995; Komuro and Rakic, 1996; Flint et al., 1999; Gomez and Spitzer, 1999). An especially well studied model system of neuronal Ca^{2+} oscillation occurs in cultured sympathetic ganglion neurons from grass frog or bullfrog that are exposed continually to caffeine or to caffeine plus depolarization (Kuba and Nishi, 1976; Smith et al., 1983; Lipscombe et al., 1988a,b; Friel and Tsien, 1992b; Friel, 1995; Cseresnyés et al., 1999). The physiological trigger for [Ca^{2+}] oscillations may be repetitive fast spiking (Peng, 1996). Most information about these oscillations has come from whole-cell fluorescence or patch-clamp recordings in which any subcellular spatial information is necessarily lost. Local Ca^{2+} regulation, however, occurs in neuronal dendrites (Finch and Augustine, 1998; Takechi et al., 1998; Koizumi et al., 1999a), contributes to the functions of some secretory cells (Pozzan et al., 1994; Thomas et al., 1996; Tse et al., 1997), and governs the direction of growth cone extension (Hong et al., 2000; Zheng, 2000). Local Ca^{2+} signaling within the soma could be equally important. Here we find evidence for local release and nonuniform propagation of Ca^{2+} in these neurons.

MATERIALS AND METHODS

Cell culture. Cultured sympathetic neurons were prepared as previously described (Cseresnyés et al., 1997). Briefly, frogs (*Rana pipiens*) were packed in ice for 20–30 min, decapitated, and pithed, according to guidelines issued by the Institutional Animal Care and Use Committee, University of Maryland (Baltimore, MD). Sympathetic ganglion chains from three frogs were removed into ice-cold Ringer's solution containing (in mM): 128 NaCl, 2 KCl, 10 glucose, 10 HEPES, pH adjusted to 7.3 with NaOH, with 0 added Ca^{2+}, manually desheathed, and enzymatically digested with 3 mg/ml collagenase for 20–40 min and then with 2 mg/ml trypsin for 7–9 min. After washing, individual cells were released from the ganglia by gentle trituration with a polished Pasteur pipette and plated onto cover glasses (VWR no. 1) coated with poly-L-lysine. Cells were maintained in culture for 2–5 d in a 50:50 mixture of Liebovitz's L-15 medium (Life Technologies, Gaithersburg, MD) with 0.1% phenol red and Ringer's solution [2 mM Ca^{2+} Ringer's supplemented with 25 μg/ml

Received March 16, 2000; revised Sept. 1, 2000; accepted Sept. 11, 2000.

This work was supported by National Institutes of Health (NIH) Grant RO1 NS33578 to M.F.S. and by NIH individual National Research Service Award NS10689 to S.I.M. We thank Dr. Christopher W. Ward for programming advice and helpful discussions.

Correspondence should be addressed to Dr. Martin Schneider, Department of Biochemistry and Molecular Biology, University of Maryland Medical School, 108 N. Greene Street, Baltimore, MD 21201. E-mail: mschneid@umaryland.edu.

Dr. McDonough's present address: Marine Biological Laboratory, 7 MBL Street, Woods Hole, MA 02543.

Copyright © 2000 Society for Neuroscience 0270-6474/00/209059-12$15.00/0

ascorbic acid, 2.5 μg/ml glutathione, 0.25 μg/ml 6,7-dimethyl-5,6,7,8-tetrahydropterine (DMPH), and 0.5 μl/ml gentamicin, pH 7.3].

Imaging. Cells were washed with 2 mM Ca^{2+} Ringer's and loaded with 2 μM fluo-4-AM (Molecular Probes, Eugene, OR) at room temperature for 20–25 min. Endogenous esterases converted nonfluorescent fluo-4-AM into fluorescent fluo-4. Culture dishes were placed on the stage of an inverted microscope (Nikon Diaphot 300) and imaged with a Nikon RCM-8000 real-time confocal microscope (Tsien and Bacskai, 1995). The focus was set at the widest area of the cell, which was at or near the vertical center. Cells were continuously superfused with a 2 mM Ca^{2+} or 0 Ca^{2+} Ringer's bath solution flowing at ~5 ml/min, and caffeine or high-K^+ Ringer's solution was microperfused onto an individual cell through a quartz perfusion head (internal diameter, 100 μm; Adams and List Associates, Westbury, NY). The internal diameter of the microperfusion pipette was approximately double the diameter of the widest part of the cell, making local caffeine gradients unlikely. The microperfusion pipette was always positioned just above the focal plane of the recorded cell image and to the left of the cell, ~50 μm away. Epifluorescent excitation for fluo-4 was with the 488 nm line of an argon-ion laser (Coherent, Santa Clara, CA), and emission was collected at $\lambda > 510$ nm. Fluo-4 fluorescence before caffeine application was mostly uniform, but often brighter in the center of the cell. Before dye loading, autofluorescence was visible in some cells as bright spots, especially in the cell center. Addition to the bath of 0.005% saponin in 0 Ca^{2+} Ringer's with 10 mM added EGTA rapidly quenched an average of 86% of the whole-cell confocal fluorescence after fluo-4 loading ($n = 4$), indicating a predominantly cytoplasmic localization of the dye. The *in vitro* K_D of fluo-4 for Ca^{2+} is 345 nM (Molecular Probes). Whole-cell peak Ca^{2+} signals measured previously with fura-2 were ~1 μM for the first and <350 nM for subsequent Ca^{2+} peaks within a caffeine-evoked oscillation cycle (Cseresnyés et al., 1999), so the fluo-4 was unlikely to be saturated.

For measurements of the direct effects of caffeine on indo-1 fluorescence (Muschol et al., 1999), neurons were loaded with 15–20 μM indo-1-AM (Molecular Probes) for 20–25 min at room temperature. Cells were pretreated with 2 μM thapsigargin (TG) (Sigma, St. Louis, MO) for at least 2 min to fully release Ca^{2+} from intracellular stores and eliminate any rise in Ca^{2+} on caffeine application (Cseresnyés et al., 1999). Excitation was at 351 nm (argon-ion laser), and emission was collected at 360 nm $< \lambda <$ 440 nm. Ca^{2+}-dependent emission from indo-1 would increase emission intensity at these wavelengths, whereas the thapsigargin-treated cells responded to caffeine with a decrease in emission intensity, verifying that a direct caffeine–dye interaction, not a Ca^{2+}–dye interaction, caused the change in fluorescence. The Ca^{2+}-independent emission obviated the need to quantify the de-esterification of indo-1-AM.

Cells were imaged with a 60× NA 1.2 water-immersion objective lens (Nikon, with correction collar to compensate for the thickness of the coverslip) to image the middle of the cell without the refractive index mismatch of an oil-immersion lens. The spatial resolution was estimated by imaging a single, 100 nm fluorescent bead in water. In the focal plane, the fluorescence intensity in the x and y directions was fit by a Gaussian function with full width at half-maximum (FWHM) of 0.3–0.4 μm. Axial (z) resolution for the confocal pinhole setting used, determined by collecting the total emission from the bead while incrementing the z position, was fit by a Gaussian function with FWHM of 1.5–2 μm. A few cells were imaged with a Nikon 40× NA 1.15 water-immersion lens. Emission values were digitized with an eight-bit converter. Data were collected at video rate with a two-frame average for an effective 15 Hz sampling rate (66 msec/frame). Images were analyzed with software custom-written in the IDL programming language (Research Systems, Boulder, CO). The whole-cell confocal fluorescence time courses are the average of unsubtracted pixel values within either the entire cell or the area indicated, except as noted. All displayed images were background-subtracted, with an average of four or five consecutive image frames acquired before changes in fluorescence. Pixels for which the averaged background image was larger than the displayed image were set to zero. Where noted, images were smoothed in space and time with a $3 \times 3 \times 3$ kernel. Smoothing was used in cells in which the subtracted signal was too dim to be apparent in still-frame images. Smoothing distorted the precise site of initiation, but made the propagation of the wave front much clearer. Grayscale shading for each pixel was set according to the look-up table bar in each figure. In the text, positions at the cell edge are sometimes referred to with "o'clock" terminology, with the position in the cell referred to by the corresponding hour hand of a clock oriented with 12 at the top.

Staining. RyRs were stained with either Bodipy FL-X ryanodine (green emission) or TR-X ryanodine (red emission) (Molecular Probes). Green emissions were recorded from 515 to 560 nm, and red emissions were recorded from 580 to 630 nm, as determined by the spectra of the excitation and emission dichroic. Cells were loaded at room temperature with 250 nM dye in Ringer's solution + 10 mM caffeine to promote high-affinity ryanodine binding to an open state of the RyR. The solution was changed to dye-free Ringer's before excitation with the 488 nm line of the argon-ion laser or with the 568 nm line of the krypton–argon laser, respectively, for the green or red emission fluorophores. The typical pattern of RyR staining around the circumference of the cell appeared after ~2 min of dye incubation. Incubation of up to 8 min resulted in brighter emission at the circumference but no increase in brightness in the interior of the cell. Mitochondria were stained with 250 nM MitoTracker Green FM (Molecular Probes) for 30 min at room temperature; the dye was washed off before imaging. For cells that were costained with MitoTracker green and TR-X red ryanodine and dually imaged, some emission from the green MitoTracker was recorded in the red channel. For cells stained only with MitoTracker green, the ratio of intensity in red divided by intensity in green for the brightest parts of the image was 0.11. Each red image taken after staining with both red ryanodine and MitoTracker green was corrected for green bleed-through by subtracting pixel by pixel with 0.11× the corresponding pixel value from the corresponding green image. There was no bleed-through of red ryanodine into the green emission channel. To stain for sarco-endoplasmic reticulum calcium ATPase (SERCA) pumps, cells were loaded with 1 μM Bodipy thapsigargin (Molecular Probes) in Ringer's solution at room temperature for 1 min, a concentration and exposure time sufficient to release Ca^{2+} from within stores and to suppress the response to 10 mM caffeine (Cseresnyés et al., 1997). After washout of TG from the bathing medium, imaging revealed discrete hot spots of fluorescence at the edges of the cell. Hot spots first appeared ~30 sec after addition of labeled TG, and the pattern was unchanged after 3 min.

Movies. Image series for selected figures (see Figs. 1, 3, 4, 7) were written as movies in Moving Picture Experts Group (MPEG) format with IDL software and are available as supplemental information for this paper. (Please see http://www.jneurosci.org.) Movies can be viewed with Windows Media Player (Microsoft, free software download available at www.microsoft.com/windows/windowsmedia/en/download/default.asp; operating system requirements listed at www.microsoft.com/windows/mediaplayer/en/download/sysreq.asp), or with other software capable of playback of MPEG files at 30 frames per second. Because images were recorded at 15 Hz, although movie playback is at 30 Hz, movies were written with a copy of each frame interleaved between each frame and the subsequent frame, so the movie gives a real-time image of Ca^{2+} spread within the cell. For the movie of Figure 7, the interoscillation period of unchanging fluorescence was cut out to conserve computer memory, and each Ca^{2+} peak was background-subtracted, with an average of five frames taken before the Ca^{2+} rise that began each individual peak.

RESULTS

Initiation of Ca^{2+} release from the cell periphery

Cell depolarization by microperfusion of a 50 mM K^+, 2 mM Ca^{2+} Ringer's solution onto a neuron evoked a fluorescence increase (Fig. 1*A*, *left*), presumably initiated by entry of extracellular Ca^{2+} into the cytoplasm through voltage-gated Ca^{2+} channels of the plasma membrane. In the confocal section, this depolarization-evoked fluorescence began as a uniform ring around the cell periphery, as expected for a uniform distribution of voltage-gated Ca^{2+} channels (Lipscombe et al., 1988a; Hernandez-Cruz et al., 1990), and then spread gradually inward (Fig. 1*B*, *image series 1*). Peak fluorescence was attained after the images shown in this series and was uniform across the cell, except for a higher emission intensity from the nucleus (Hernandez-Cruz et al., 1990; Perez-Terzic et al., 1997). Instead of a higher nuclear Ca^{2+} concentration, this is likely to reflect a different solvation environment for the fluo-4 dye in nuclear and non-nuclear compartments (Perez-Terzic et al., 1997). Fluorescence decayed to baseline levels after returning the cell to Ca^{2+}-free Ringer's solution. Full Ca^{2+} removal was confirmed by the lack of fluorescence increase evoked by microperfusion of 50 mM K^+, 0 Ca^{2+} Ringer's (Fig. 1*A*, *center*).

Cytoplasmic Ca^{2+} levels were also increased by evoking release of Ca^{2+} from intracellular stores. Efflux via RyRs was evoked pharmacologically by microperfusion of 10 mM caffeine. In this cell, application of caffeine in Ca^{2+}-free Ringer's solution evoked a fluorescence increase (Fig. 1*A*, *right*), consistent with whole-cell studies showing that extracellular Ca^{2+} is not required for the release of Ca^{2+} from intracellular stores (Neering and McBurney, 1984; Lipscombe et al., 1988a; Thayer et al., 1988; Friel and Tsien, 1992a; Cseresnyés et al., 1997, 1999). Cytoplasmic Ca^{2+} is a physiological ligand for RyRs. Caffeine increases RyR Ca^{2+} sensitivity, possibly analogous to the effects of cyclic ADP-ribose or other modulatory pathways (Rousseau et al., 1988; Sitsapesan and Williams, 1990; McPherson et al., 1991; Hua et al., 1994; Empson and Galione, 1997), thereby allowing the Ca^{2+} release at resting Ca^{2+} levels observed here. Ca^{2+} stores governed by $InsP_3$ receptors, if present at all in these amphibian neurons, are labile and quite small compared with the stores governed by RyRs (Pfaffinger et al., 1988; Friel and Tsien, 1992a) (but see Kirkwood et al., 1991). We cannot, however, exclude the possibility that the Ca^{2+} signal includes some component of Ca^{2+} release through $InsP_3$Rs.

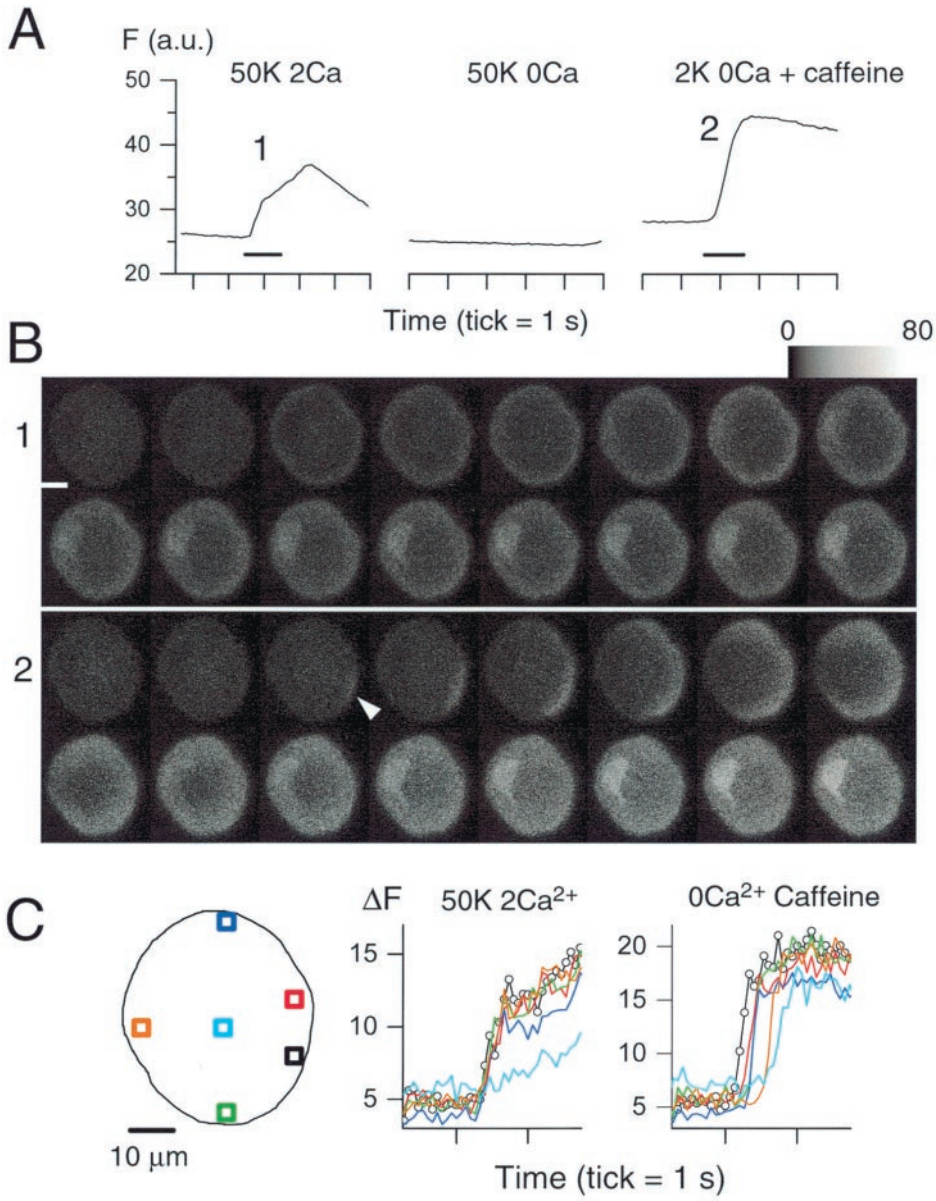

Figure 1. Caffeine evokes release of Ca^{2+} from a discrete site at the cell edge. For this cell, the continuously flowing bath solution was frog Ringer's solution without added Ca^{2+}. *A*, Time course of confocal fluorescence averaged from within the entire cell in response to microperfusion of Ringer's solution containing 50 mM K^+ and 2 mM Ca^{2+} (*left*, *trace 1*); 50 mM K^+ and zero added Ca^{2+} (*middle*); and 2 mM K^+, 0 Ca^{2+} with 10 mM caffeine (*right*, *trace 2*). There is a 2 min interval between the *left* and *middle panels*, sufficient time for recovery of responsiveness to high-K^+ stimulation (Friel and Tsien, 1992a), and a 1 min interval between the *middle* and *right panels*. *B*, *Image series 1* and *2* are consecutive images taken from the areas under *traces 1* and *2* in *A*, marked with the *horizontal bars*. The *arrow* in *image series 2* indicates the site of fluorescence initiation. Pixel values from 0 to 80 were assigned brightness according to the *grayscale look-up bar*. Scale bar, *image series 1*, 10 μm. *C*, Time course of the fluorescence in small subcellular areas during depolarization and caffeine application. *Left*, *Map* of the cell showing the subcellular areas from which the fluorescence signal in *A* was further analyzed. *Right*, Time course of the change in fluorescence (arbitrary units) within the subarea of the corresponding color at the onset of fluorescence of *traces 1* (50K) and *2* (caffeine). *Open circles*, shown only for the black subarea, indicate the sampling interval of 66 msec. Each tick on the *x*-axis is 1 sec. Scale bar, 10 μm. Please see associated movie of the responses to 50 mM K^+ and to caffeine (*B*) in the electronic version of this paper.

The caffeine-evoked increase in Ca^{2+}-dependent fluorescence began at a single discrete site on the right edge of the cell, presumably at the low side of any caffeine gradients attributable to microperfusion from the left (Fig. 1*B*, *image series 2*). From the site of release, the Ca^{2+} spread around the cell periphery, faster in the counterclockwise than the clockwise direction, followed by radial spread into the center (Fig. 1*B*, *image series 2*, *C*, *right*). Ca^{2+} reached different sites around the cell edge with a delay, but without decrement of the amplitude (Fig. 1*C*). The rise of fluorescence at each peripheral location was rapid, going from baseline to a near-maximal change in two or three images (66 msec/image). From the difference in the time to half-maximal fluorescence at the release initiation site (*black*), at the cell periphery opposite the origin (*orange*), and at the cell center (*light blue*), the one-dimensional speed of Ca^{2+} propagation with caffeine can be estimated as 130 μm/sec clockwise and 230 μm/sec counterclockwise around the cell periphery, and 40 μm/sec radially inward. Because free Ca^{2+} would be expected to diffuse decrementally in all directions from a single release site, much of the Ca^{2+} propagation must have been caused by a process other than passive diffusion. This process was likely regenerative calcium-induced calcium release (CICR) among RyRs distributed through the cell. In eight neurons, with caffeine, the circumferential propagation speed averaged 204 ± 39 μm/sec, and radial propagation averaged 49 ± 6 μm/sec ($p < 0.012$; unpaired *t* test). Assuming minimal anisotropies in the diffusion path for Ca^{2+} in the cytoplasm, the slower radial propagation implies a greater propensity for CICR around the periphery than toward the center of the cell. In the cell of Figure 1, the speed of inward propagation during depolarization without caffeine (*image series 1*) was 20 μm/sec. This is only an upper bound on the rate of Ca^{2+} diffusion because Ca^{2+} elevation during depolarization evokes a degree of CICR even in the absence of caffeine (Friel and Tsien, 1992a; Hua et al., 1993, 1994; Llano et al., 1994; Shmigol et al., 1995; Peng, 1996; Usachev and Thayer, 1997). In the same eight neurons, inward radial propagation speed in response to high-K^+ depolarization was 26.9 ± 6.2 μm/sec, whereas inward radial propagation in the same cells during subsequent exposure to 10 mM caffeine, after return to baseline fluorescence in Ringer's solution, measured as 49.0 ± 6.9 μm/sec ($p < 0.02$). The ratio of speed in caffeine to speed in high-K^+ was 2.5 ± 0.5.

The caffeine dependence of propagation speed was tested by evoking Ca^{2+} release first with 5 mM and then, after washout, with 20 mM caffeine. In three of three cells, Ca^{2+} release originated at the same peripheral site with 20 mM as with 5 mM; in one of the three cells, release was also seen from a second site. The one-dimensional peripheral propagation speed evoked by 5 and 20 mM caffeine applied to each of the former two cells increased from ~90 to ~430 μm/sec and from ~100 to ~350 μm/sec. Because the

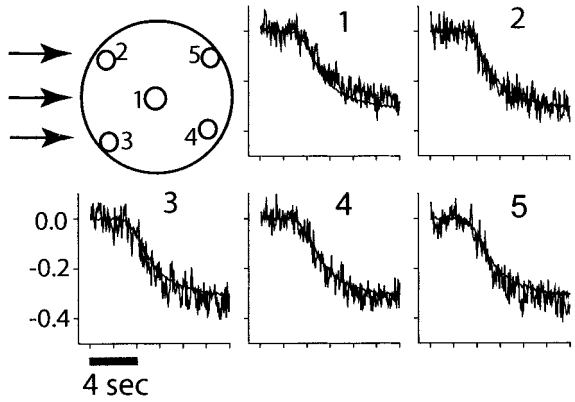

Figure 2. Time course of caffeine spread within a cell. The decrease in indo-1 emission intensity on caffeine application was used to detect the time course of caffeine within a thapsigargin-treated cell (see Materials and Methods). *Top left*, *Outline* of a cell and of five arbitrarily chosen *subareas* within the cell. *Arrows* to the *left* of the *cell outline* show the direction of external caffeine microperfusion. In each *numbered panel*, the fractional change in average fluorescence within the correspondingly *numbered subarea* (noisy *trace*) is plotted together with the fractional change in fluorescence averaged from within the entire cell (less noisy *trace*, mostly superimposed on the subarea fluorescence). Each tick on the *x*-axis represents 2 sec. The decay for each subarea was fit well by a single Boltzmann function. The 50% decay time for each subarea minus the 50% decay time for the whole cell average was as follows: area 1, +82 msec; area 2, −198 msec; area 3, −208 msec; area 4, −47 msec; area 5, −55 msec.

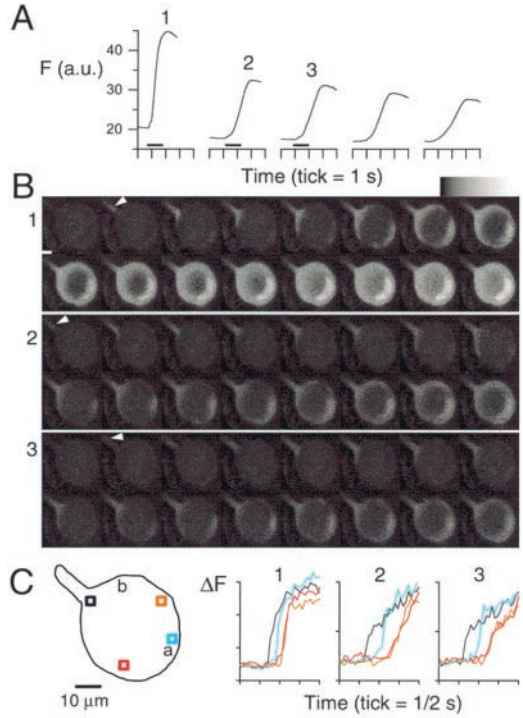

Figure 3. Origin and spread of intracellular Ca^{2+} in response to successive applications of caffeine. *A*, Time course of average fluorescence within the entire cell in response to five successive applications of 10 mM caffeine. Record is discontinuous between caffeine applications; fluorescence returned to baseline in the interpeak intervals. *B*, Consecutive confocal images corresponding to the indicated intervals (*A, bars*) during the upstroke of each of the first three peaks in the whole-cell confocal fluorescence time course. The *grayscale look-up bar* represents pixel values from 0 to 80. *Arrow* in each image series indicates the point of first increase in fluorescence on stimulation with caffeine. Scale bar, 10 μm. *C*, *Left*, *Outline* of the cell, with labeled arbitrary subareas marked with *boxes*, and arbitrary spatial reference points *a* and *b*. *Right*, Time course of fluorescence during the first three caffeine applications within the subarea defined by the correspondingly *colored box*. Each tick on the *y*-axis represents 10 arbitrary fluorescence units calculated from background-subtracted images (note different scale for different caffeine applications). Please see associated movie of the first three caffeine applications to this cell (*B, 1–3*) in the electronic version of this paper.

concentration and mobility of dye and of endogenous buffers was the same for both applications of caffeine, the increase in speed can be attributed to an increased fraction of CICR.

Spread of intracellular caffeine

At a given intracellular location, the local cytoplasmic concentrations of caffeine and fluo-4, as well as Ca^{2+}, influence the observed fluorescence signal. The proportion of a given area that is occupied by cellular organelles, and thus effectively inaccessible to the dye, would also affect emission intensity. Detection of fluorescence itself confirms the presence of fluo-4 in a given area, whereas the homogenous increase of cytoplasmic fluorescence during peak responses to caffeine (Figs. 1, 3, 7, 9) provides some evidence against gross inequalities in fluo-4 distribution among different regions of the cytoplasm at this resolution. Because caffeine must diffuse across the plasma membrane and through the intracellular milieu to act on RyRs of the ER membrane, the recorded fluorescence could reflect regional differences in caffeine, not Ca^{2+}. To monitor intracellular caffeine levels during external application of caffeine, fluorescence of cells loaded with the dye indo-1 was measured in response to extracellular microperfusion of 10 mM caffeine. Cells were pretreated with thapsigargin to eliminate Ca^{2+}-dependent fluorescence (see Materials and Methods). Caffeine reduced the intracellular indo-1 fluorescence emission intensity at 360 nm $< \lambda <$ 440 nm, wavelengths at which Ca^{2+} binding increases indo-1 emission intensity. Thus we attributed the decrease in emission to a direct caffeine-dye interaction (Muschol et al., 1999) and used it to measure the penetration of caffeine within the cell. Figure 2 shows the magnitude and time course of indo-1 fluorescence averaged over the entire outline of a cell image and from within each of five numbered, arbitrarily chosen subareas. Each panel shows on the same scale the change in fluorescence from the correspondingly numbered subarea (noisy solid line) and from the entire cell (less noisy line) in response to the same caffeine application. The total amplitude decrease was the same for all subareas. The time to 50% decay was shortest at the left side of the cell, closest to the caffeine application, and slowest in the middle (Fig. 2, legend), but the greatest difference in time between any two subareas was 290 msec. In results pooled from the two left and two right subareas of three cells, the 50% decay time was reached more quickly than the whole-cell average, by 159 ± 84 msec at the left side and by 29 ± 34 msec at the right side (mean ± SD; $n = 6$). The decay time at the center of the cell (subarea 1) was 92 ± 8 msec slower than the whole-cell time course (mean ± SD; $n = 3$). We conclude that caffeine permeates the membrane rapidly in these cells and equilibrates with only minor differences among different regions of the cell. This further implies that the local signaling events that were observed reflected elevations of intracellular Ca^{2+}, and not caffeine. In a different cell, release of Ca^{2+} from a discrete site at the cell edge was observed ~20 min after bath application of caffeine (data not shown), obviously well after equilibration of intracellular caffeine.

Sites of preferential Ca^{2+} release

Propagation of elevated Ca^{2+} via regenerative CICR suggests that many sites throughout the cell are capable of releasing Ca^{2+}. Caffeine was applied multiple times to a single cell to test whether the site of initial release was random, or whether it might reflect functional differences among RyRs (Fig. 3). In response to each caffeine application, fluorescence increased first at a discrete site in the distal part of a growth cone and propagated from there into the cell body. Because the base of the growth cone was in the same focal plane as the cell body, for this cell the actual initial Ca^{2+} increase in the cell body occurred unambiguously within the recorded confocal section. Although Ca^{2+} increases were eventually recorded from the entire intracellular area, significant nonuniformities in fluorescence initiation and spread occurred well after the ~0.5 sec required for caffeine to reach all points within the cell,

providing evidence for functional differences among stores. Before the increase from the growth cone had extended over the entire perimeter of the cell, another localized increase in fluorescence was observed at arbitrarily labeled site "*a* " at the right edge of the cell (*blue box*), opposite the direction of caffeine microperfusion, without Ca^{2+} increases in the intervening regions (Fig. 3*C*). In addition, whereas Ca^{2+} spread smoothly from the base of the growth cone symmetrically in the clockwise and counterclockwise directions during the first caffeine application, Ca^{2+} spread much more slowly after subsequent caffeine applications, especially in the radial and clockwise directions. These same patterns of initiation and propagation were recorded for each of five separate caffeine applications to the cell (Fig. 3), further supporting the idea that the site (or sites) where release initiates is not random, but rather an intrinsic Ca^{2+} release property of the site itself.

Caffeine was applied to a total of 67 cells in either Ca^{2+}-free or 2 Ca^{2+} Ringer's solution. In 47 cells, the increase in fluorescence began at one or more discrete sites, always at the edge of the cell. Conceivably, a tonic influx of external Ca^{2+} might have resulted in a higher cytoplasmic Ca^{2+} concentration near the plasma membrane, and consequently in easier CICR at the cell edges, but the lack of a requirement for Ca^{2+} influx for caffeine-evoked Ca^{2+} release argues against this (Fig. 1) (Neering and McBurney, 1984; Lipscombe et al., 1988a; Thayer et al., 1988; Friel and Tsien, 1992a; Cseresnyés et al., 1997, 1999). The initial Ca^{2+} release was at the left side of the cell in 32 of 47 cells, presumably reflecting a transiently higher caffeine concentration closer to the microperfusion pipette (Fig. 2). Increase initiated at the right side of the cell (Fig. 1), opposite to the direction of caffeine application, in 5 of 47 cells. (In seven cells, release initiated from both the left and right sides of the cell, and in three cells release initiated from the top or bottom of the imaged plane of the cell.) This suggests differences in caffeine sensitivity among different release sites (see Discussion).

In 20 of 67 cells, caffeine caused a fluorescence increase that occurred with a diffuse pattern, arising either simultaneously across the entire cell, or from diffuse bands extending more than one-fourth of the way around the cell perimeter (data not shown). In these cells, the actual Ca^{2+} release could have occurred simultaneously throughout the cell, as recorded, or could have propagated from a single release site outside the focal plane to appear as a more uniform rise of Ca^{2+} in the recorded plane. Because release from discrete sites in a three-dimensional cell would sometimes be expected to appear in two-dimensional confocal recordings as a diffuse rise, we prefer the explanation that actual Ca^{2+} release was always from a discrete site, rather than invoking different release mechanisms among neurons of the same type. This interpretation is supported by a recording of three consecutive caffeine applications to the same cell made with the focal plane set to the center of the cell ($z = 0$), to 8 μm above the center ($z = +8$), and to 8 μm below the center ($z = -8$). With the focus at $z = 0$, the Ca^{2+} release initiated from a broad band covering the top half of the image; at $z = +8$, release initiated from a small site several micrometers wide at ~11 o'clock on the cell edge; and at $z = -8$, release initiated evenly over the entire confocal image (data not shown). The patterns observed at each focal plane are consistent with initiation of Ca^{2+} release from a discrete site at $z = +8$ on each caffeine application. Assuming that successive caffeine applications evoked Ca^{2+} release from the same site each time, as in the cell of Figure 3, this suggests that the diffuse patterns of Ca^{2+} release recorded from 20 cells were caused by propagation from a discrete release site that was out of focus.

Sites of Ca^{2+} release during oscillations in intracellular Ca^{2+} levels

To determine whether discrete sites of release were maintained during oscillations in cytoplasmic Ca^{2+} levels (Lipscombe et al., 1988a,b; Friel and Tsien, 1992b; Friel, 1995; Cseresnyés et al., 1999), oscillations were evoked by steady microperfusion of 10 mM caffeine in 2 mM K^+, 2 mM Ca^{2+} Ringer's solution. The amplitude of each peak decreased during the oscillation train. This decrease

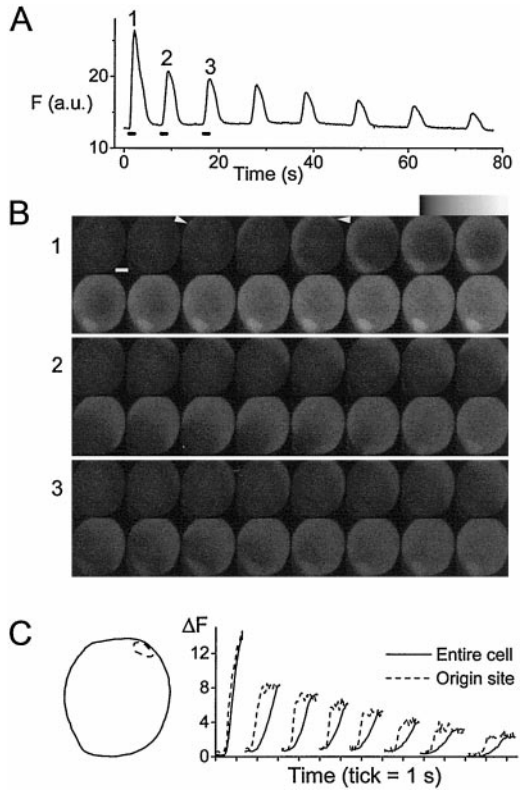

Figure 4. Patterns of Ca^{2+} during caffeine-evoked oscillations. *A*, Time course of whole-cell confocal fluorescence in response to continual microperfusion of 10 mM caffeine. *B*, Consecutive confocal images corresponding to the indicated intervals (*A, bars*) during the upstroke of each of the first three peaks in the oscillation cycle. *Arrows* show initiation sites of Ca^{2+} release. Scale bar, 10 μm. *C*, Time course of fluorescence at the onset of each oscillation peak for the whole cell (*solid line*) and for the marked subcellular area (*dashed line*). The interpeak regions of unchanging fluorescence have been removed to display the upstroke of each oscillation peak at an expanded time scale; the decay of fluorescence after each peak is not shown. The *y*-axis represents the change in fluorescence with time; minimum fluorescence values for the unsubtracted whole-cell (12.5) and origin site (10.2) time courses are subtracted from the displayed time courses. Please see associated movie displaying the oscillation series in real time in the electronic version of this paper.

was also seen in whole-cell recordings exhibiting decreasing oscillations monitored with the ratiometric Ca^{2+} indicator fura-2 (Cseresnyés et al., 1999), so the records here may reflect actual decreases in Ca^{2+} levels rather than photobleaching of the fluo-4. Because caffeine was applied continuously to evoke oscillations, patterns of Ca^{2+} release after the first Ca^{2+} peak occurred in the presence of a uniform intracellular caffeine concentration. Figure 4 displays images from a cell that responded to continual caffeine application with a cycle of eight oscillation peaks (*A*). For the first peak, fluorescence increase was first observed over an area ~2 × 2 μm at ~11 o'clock (*B*, *image series 1*, *frame 3*, *arrow*) and spread from there. Fluorescence increased two frames (132 msec) later at a second site, at ~2 o'clock (*B*, *image series 1*, *frame 5*, *arrow*). For each of the seven subsequent Ca^{2+} peaks in the oscillation cycle, fluorescence increased at that same 2 o'clock site before increasing in the rest of the cell (Fig. 4*B*, *image series 2, 3*; *C*; *movie*). Fluorescence at the release site increased and then stayed constant during the rising phase of the whole-cell fluorescence (Fig. 4*C*), suggesting that Ca^{2+} release was completed at the initiation site as the wave front propagated. Release did not initiate again from the first (11 o'clock) site, suggesting that release at that site reflected proximity to the direction of caffeine application. Thus, the timing of a cell-wide Ca^{2+} increase during Ca^{2+} oscillations was determined by Ca^{2+} release at a single site. These neurons appear to have an "oscillator" site at the cell edge from which release initiates, as reported for $InsP_3$-evoked Ca^{2+} oscillations in some

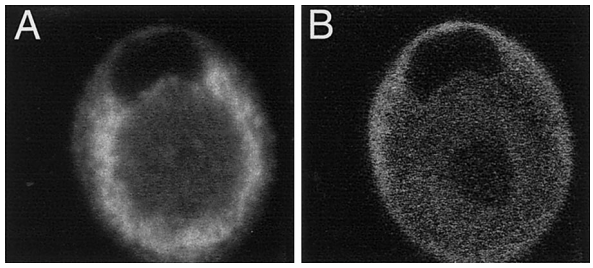

Figure 5. Localization of ryanodine receptors and mitochondria. Representative cell exposed to both MitoTracker and to a fluorescent analog of ryanodine. *A*, *Green emission*, corresponding to mitochondria. *B*, *Red emission*, corresponding to ryanodine. Images were corrected for a small bleed-through of the *green emission* into the *red channel* as described in Materials and Methods.

nonexcitable cells (Rooney et al., 1990; Pozzan et al., 1994). In all neurons recorded, each rise in Ca^{2+} at the oscillator site was followed by extension of a Ca^{2+} wave front farther into the cell. Mitochondrial Ca^{2+} stores do not initiate Ca^{2+} oscillations in these neurons (Friel, 1995), suggesting that the observed oscillator sites reflected Ca^{2+} release from ER, rather than mitochondrial stores. The wave front propagated first around the cell edges and then radially inward for each peak in the oscillation. For this cell, final fluorescence in any oscillation was as bright in the center of the cell as at the periphery. Considering the combined second, third, and fourth oscillation peaks from each of five cells, the ratio of radial to circumferential propagation speed was 0.18 ± 0.05 ($n = 15$; mean ± SEM). For six oscillation peaks, radial propagation failed entirely (speed = 0); excluding those, the ratio of radial to circumferential propagation speed was 0.29 ± 0.05 ($n = 9$). Thus, on average, the circumferential propagation speed was more than threefold greater than the radial propagation speed, measured with a uniform intracellular caffeine concentration. The off-rate of Ca^{2+} from fluo-4 [measured for fluo-3 as 424 sec^{-1} by Lattanzio and Bartschat (1991), and 175 sec^{-1} by Escobar et al. (1997)] is likely to be too rapid for any anisotropies in the fluo-4 diffusion pathway to have delayed the radial spread of Ca^{2+} to this extent.

Molecular correlates of initiation and propagation

Functional measurements presented above show that when discrete sites of Ca^{2+} release are observed, they are always at the cell edges, and that the Ca^{2+} wave front propagates faster around the circumference of the cell than radially inward. To explore a possible organellar or molecular basis for these observations, living neurons were stained with fluorescent analogs of ryanodine and thapsigargin and with MitoTracker to detect intracellular distributions of RyRs, SERCA pumps, and mitochondria. Figure 5 shows images from the same cell simultaneously labeled with green-emitting MitoTracker (Fig. 5*A*) and with red-emitting ryanodine (Fig. 5*B*), recorded at two different emission wavelengths (see Materials and Methods). Images of all neurons (Table 1) taken with labeled ryanodine showed a bright ring around the cell circumference (Fig. 5*B*), independent of the length of time of dye incubation ($n = 5$). Mitochondria similarly exhibited a ring of brighter fluorescence within all cells (Fig. 5*A*; $n = 7$), a wider ring that extended to the inner margin of the bright ring observed with labeled ryanodine. Neither marker stained the nucleus (Fig. 5, *dark crescent* at *top*). Autofluorescence was always negligible compared with fluorescence because of staining for RyRs or mitochondria. Apparently, the density of RyRs is heavier in the circumference of the cell than in the interior, and the vast majority of mitochondria are localized in an inner ring just inside the RyRs. These distributions held when the entire cell was imaged with a series of confocal sections taken at incremented focus settings (data not shown). The presence of RyRs at the cell edge suggests an obvious molecular basis for the initiation of caffeine-evoked Ca^{2+} release at the cell edge. Possibly RyRs are only available on the cell edge, or those at the cell edge have greater sensitivity to caffeine. However, the non-zero inward radial spread of Ca^{2+} (via CICR) suggests functional RyRs throughout the cell. More likely, the higher RyR density at the edge of the cell increases the likelihood that a unitary Ca^{2+} release event through an RyR at the cell edge will induce Ca^{2+} release from neighboring RyRs, and so initiate a regenerative wave front. The distributions of both RyRs and mitochondria might also explain the slower radial propagation of Ca^{2+} wave fronts. A regenerative Ca^{2+} wave front would be expected to travel faster along a path of higher RyR density because Ca^{2+} released from one RyR or RyR cluster has a shorter distance to diffuse to and activate neighboring clusters than when RyRs are less dense. In addition, mitochondria in these neurons serve as active Ca^{2+} stores (Friel and Tsien, 1994; Pivovarova et al., 1999); uptake of Ca^{2+} into mitochondrial stores would be expected to buffer the speed of radial, but not circumferential, Ca^{2+} propagation.

Although RyRs were located at the cell perimeter, staining with labeled ryanodine did not reveal clusters of RyRs that might correspond to the sites that repeatedly initiated Ca^{2+} release. Staining with labeled thapsigargin, however, provided a possible molecular correlate. Thapsigargin binds to (and inhibits the function of) SERCA pumps, a major mechanism for reuptake of cytoplasmic Ca^{2+} into intracellular stores in these neurons (Cseresnyés et al., 1997). Living neurons exposed to a brief pulse of labeled TG followed by washout of TG showed hot spots at the cell edges (Fig. 6*A*,*C*,*E*,*F*), corresponding to spots with a higher density of SERCA pumps. Longer exposures to labeled TG increased emission intensity at the hot spots, but not at other intracellular areas. Such focal peripheral fluorescence was seen in 11 of 14 cells stained with the fluorescent TG. Autofluorescence was significant compared with TG staining in some cells (Fig. 6*D*) but not in others (Fig. 6*B*). However, the autofluorescence always consisted of discrete spots in the interior of the cell, clearly different from the peripheral focal fluorescence seen after staining with fluorescent TG. The position of the autofluorescent spots changed with time in these unfixed cells, possibly reflecting movement of intracellular organelles, thus precluding the ability to correct for autofluorescence by subtracting the background image. Assuming that the TG-labeled pumps in the hot spots are functional, a higher density of SERCA pumps might be expected to result in locally higher Ca^{2+} concentrations within the adjoining intracellular stores for the condition of steady-state pump leak balance. Higher levels of stored Ca^{2+} are known to make RyRs more likely to open in response to a given level of cytoplasmic Ca^{2+} (Gyorke and Gyorke, 1998; Koizumi et al., 1999b). We speculate that a high density of SERCA pumps results in locally high Ca^{2+} levels within the stores, which in turn makes the apposed RyRs more likely to open in response to caffeine application.

Multiple release initiation sites during Ca^{2+} oscillations

In 7 of the 14 cells that oscillated in response to steady caffeine application, release for each peak after the first initiated from a single site, as in Figure 4. For three cells, the Ca^{2+} rise was homogenous over the entire confocal section, without detectable spatial anisotropy (data not shown). In four cells, however, oscillation peaks originated from more than one discrete site; release of Ca^{2+} was observed from four separate release sites for the cell displayed in Figure 7 (see Fig. 7, *movie*). This cell responded to steady caffeine application with 28 fluorescence peaks (Fig. 7*A*). In this cell, the oscillation peaks initiated from multiple sites simultaneously or from different single sites, all located at the cell edge. Image series (Fig. 7*B*) and fluorescence amplitudes from within four arbitrarily located sites (Fig. 7*C*,*a–d*) for five oscillation peaks with different patterns of release initiation are shown. The first peak in the oscillation originated only from a band at the left edge (Fig. 7*B*, *image series 1*). For most oscillation peaks, Ca^{2+} rose at the different sites within a few frames of each other or simultaneously, as in the fourth peak (*image series 4*). Late in the oscillation cycle, however, Ca^{2+} levels at the different sites increased with time lags of up to 2 sec, reflecting release initiation from different points. The first Ca^{2+} increase (Fig. 7) was near area *c* for peak 23,

Table 1. Summary of calcium release and propagation properties for all cells analyzed and the number of cells from which staining measurements were made

Cells with recorded caffeine-evoked Ca^{2+} release	67
Cells with discrete release sites in the recorded optical section	47
Cells with a single discrete initial release site on the left side	32 of 47
Cells with a single discrete initial release site on the right side	5 of 47
Number of cells that oscillated	14
Oscillating cells with a discrete release site in the recorded optical section	11
Oscillating cells with only one discrete release site in the recorded optical section	7
Radial propagation speed upon depolarization/speed upon first caffeine application	0.41
Radial propagation speed/circumferential speed with caffeine during oscillations	0.29
Cells with circumferential pattern of ryanodine stain	5 of 5
Cells with ring pattern of mitochondrial stain	7 of 7
Cells with punctate edge pattern of thapsigargin stain	11 of 14

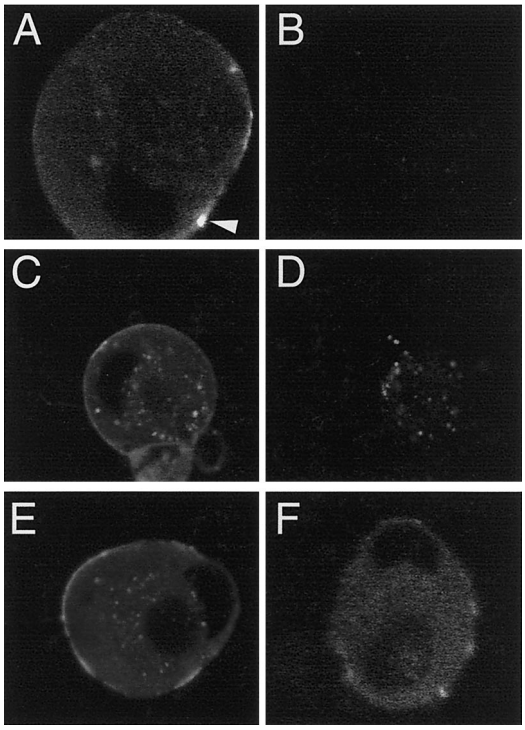

Figure 6. Localization of SERCA pumps. Confocal images of cells exposed briefly to a fluorescent analog of TG (see Materials and Methods). Pixel values were fit to a linear grayscale. *A*, Cell after TG staining. Scaling factor was chosen to highlight contrast through the entire cell. The *arrow* points to an area of especially intense staining that was far offscale after scaling. Thus, the picture understates the contrast between this hot spot and the rest of the cell. *B*, Background fluorescence of the same cell as *A*, with the same scaling. The *image* was taken before exposure to TG. *C*, A different cell after TG exposure. *D*, Background fluorescence of the same cell as *C*, with the same scaling. The *image* was taken before exposure to TG. *E*, *F*, two additional cells, *images* taken after TG exposure.

near area *d* for peak 26, near area *b* for peak 27 (*image series 23*, *26*, and *27*), and near area *a* for peak 28 (see *movie*). Ca^{2+} never increased first near the 12 o'clock position in this cell, although fluorescence clearly spread to and through this area without discontinuity for each peak in the oscillation cycle. Either several different sites along the cell edge can act as an oscillator site to initiate cell-wide Ca^{2+} release, or Ca^{2+} propagation from a single, out-of-focus release site explains the different patterns. Such propagation would have to be different enough for different peaks within the oscillation cycle to appear in the recorded optical section, sometimes as simultaneous release from sites *a–d*, and sometimes as release from just one of each of the four sites in turn.

It is easy to imagine how regular discharge of a single release initiation site could produce a regular overall oscillation frequency. Interestingly, however, in the four cells in which different oscillation peaks originated from different release initiation sites (Fig. 7), the oscillation frequency was also regular, with only a monotonic decline in frequency with time (Cseresnyés et al., 1999). It might have been expected that stochastic release from several active initiation sites would sometimes produce an overall oscillation record with irregular interpeak intervals. Moreover, cells with more functional release initiation sites might oscillate at a higher overall frequency. Figure 8 shows oscillation frequency as a function of the number of separate initiation sites for each oscillating cell with a discrete initiation site of Ca^{2+} release. Oscillation frequencies were comparable with those evoked in intact nerve terminals by 20 Hz firing (Peng, 1996). No correlation was evident between oscillation frequency and the number of initiation sites. One interpretation is that a wave front extending throughout the cell via CICR discharges the Ca^{2+} stores at all possible release initiation sites, thereby eliminating the possibility of independent initiation of two oscillation peaks in close succession from different release initiation sites.

Propagation of the Ca^{2+} wave front

Spread of the fluorescence wave front was observed to fail not only in certain intracellular directions, as in Figure 3, but also across the entire cell. Failures occurring within an oscillating cell were the most informative because wave fronts that extended successfully throughout the same cell confirmed the presence of dye and active Ca^{2+} stores. Such a cell is shown in Figure 9. For this cell, each oscillation peak after the first originated from a site at ~4 o'clock on the cell edge (Fig. 9*C*, *arrows*). From this site, fluorescence spread over the entire cell for peaks 1–5, 7, and 9 within the oscillation cycle, but failed to extend fully into the left side of the cell for peaks 6, 8, and 10. The propagation failure is reflected in the smaller signal for these peaks in the whole cell confocal record (Fig. 9*A*). Such failures probably underlie the "small oscillations," that were frequently observed, especially late in an oscillation cycle, in whole-cell studies of caffeine-induced Ca^{2+} oscillations in these neurons (Cseresnyés et al., 1999). Thus, propagation failure is likely quite common.

Figure 9*B* shows quantitatively the fluorescence spread over two arbitrarily defined rectangular areas of this cell for the seventh, eighth, and ninth oscillation peaks. For the seventh and ninth oscillation peaks, fluorescence increased first within the *right rectangle* (*solid line*), close to the 4 o'clock initiation site, then slightly later in the *left rectangle* (*dashed line*). For the eighth peak, however, fluorescence increased in the *right rectangle* but stayed at baseline levels in the left rectangle. Consecutive confocal images from the eighth oscillation peak illustrate the failure of the wave front to extend from the initiation site into the *left side* of the cell (Fig. 9*C*). Oscillation peak 6 spread over perhaps three-fourths of the cell, whereas peaks 8 and 10 propagated only approximately halfway. The continuous decline in fluorescence between oscilla-

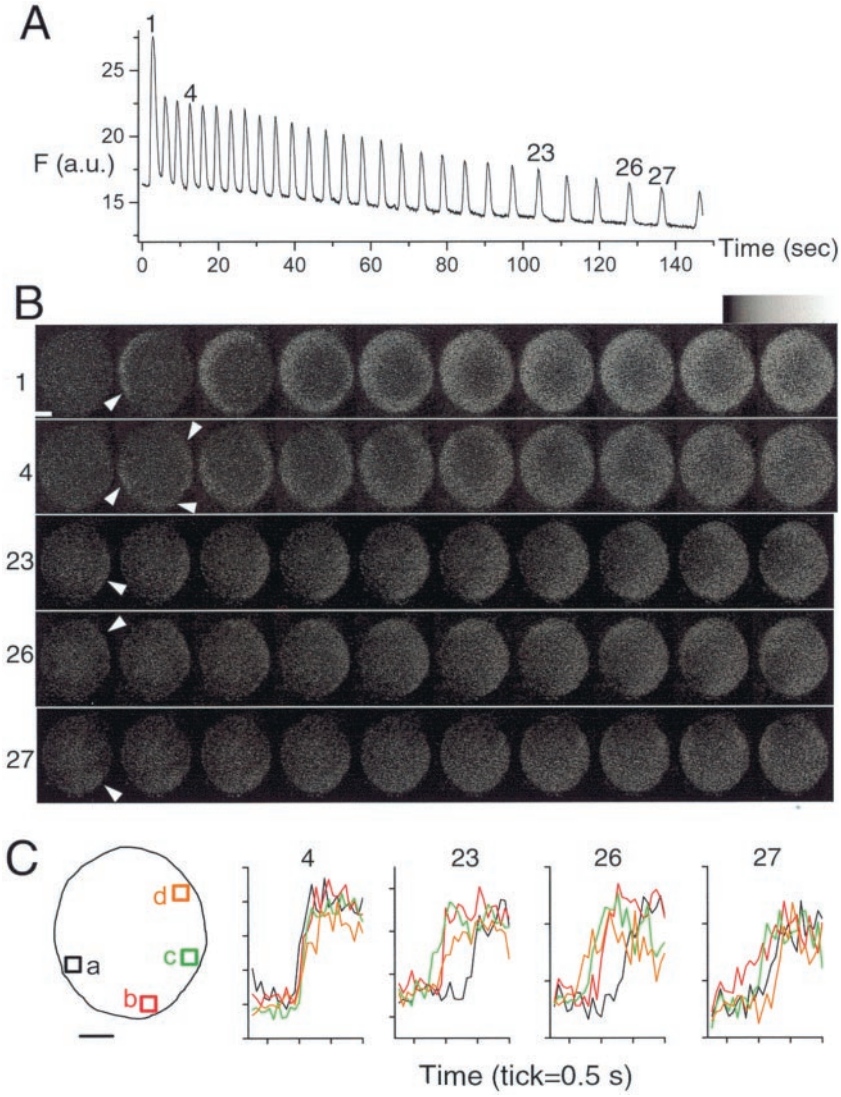

Figure 7. Ca^{2+} oscillations from a cell with multiple initiation sites of release. *Top*, Time course of fluorescence averaged from within the whole cell confocal plane in response to continual microperfusion of 10 mM caffeine. *Oscillation peaks 1, 4, 23, 26*, and *27* are labeled to correspond to the image series below. *B*, Consecutive confocal images from the upstroke of *oscillation peaks 1*, *4*, *23*, *26*, and *27*. Scale bar, 10 μm. In each peak, fluorescence spread from the initiation site over the entire cell; the final stages of spread are not shown to conserve space. *Arrows* indicate sites of release initiation for each displayed oscillation peak. The *look-up bar* represents pixel values from 0 to 70 for *oscillation peaks 1* and *4*, and 0 to 50 for *oscillation peaks 23, 26,* and *27*. *Image series 23, 26,* and *27*, where the fluorescence signal was much dimmer, are smoothed for clarity. *Image series 1* and *4* are unsmoothed. *C*, Time course of fluorescence within subareas at the four different release initiation sites. *Left*, *Outline* of the cell, with *boxes a, b, c,* and *d* arbitrarily placed to reflect the different initiation sites of Ca^{2+} release. *Right*, Time course of average pixel values within the *boxes* of corresponding color for *oscillation peaks 4, 23, 26,* and *27*. Each tick on the *x*-axis represents 0.5 sec; each *tick* on the *y*-axis represents an increase of 2 arbitrary fluorescence units measured from background-subtracted images (note different scale for different peaks). Please see associated movie of the smoothed compacted record of the entire oscillation series, with the inter-oscillation times cut out to conserve memory, in the electronic version of this paper.

tion peaks in Figs. 7, 9, and 10 probably indicates continuous photo bleaching of the fluo-4 in these cells during the prolonged recording time. What caused the propagation failures observed here? After oscillation peaks 5, 7, and 9, Ca^{2+} decreased simultaneously in the left and right sides of the cell. This suggests that the stores on the left side had indeed reloaded Ca^{2+} that was then available for release during peaks 6, 8, and 10. A failure of stores to release accumulated Ca^{2+} likely caused the wave to stop, although other modulations are possible. Failure of RyRs to open could have been caused by insufficient levels of either cytoplasmic or lumenal Ca^{2+} (Gyorke and Gyorke, 1998; Koizumi et al., 1999b).

The observed propagation of the Ca^{2+} wave front represents the sum of contributions from passive diffusion of free Ca^{2+}, diffusion of Ca^{2+} complexed with fluo-4 or endogenous buffers, and propagation attributable to CICR. Presumably caffeine selectively increases the amount of spread attributable to CICR. Although pharmacological interventions that inhibit CICR would also inhibit the initial Ca^{2+} release, several points argue that the spread of Ca^{2+} wave fronts in the presence of caffeine was almost wholly attributable to CICR. The propagation failures illustrated in Figure 9, in which the Ca^{2+} wave front was stationary for ~1 sec in an area that contained dye and active stores, suggest a minimal role for diffusion (see also Fig. 10). Moreover, we observed Ca^{2+} increases with similar rise time and peak amplitude at various distances from the point of initial release (Figs. 1*C*, 3*C*, 7*C*). Passive diffusion would have resulted in increasingly delayed and decremental increases in free Ca^{2+} with increasing distance from the Ca^{2+} source.

Decay of Ca^{2+} levels

For most cells, the decay of fluorescence after either depolarization or caffeine application was uniform across the cell (see *movies*). Nuclear fluorescence decayed with the same time course as cytoplasmic fluorescence, measured for the cell in Figure 4 (data not shown). Subcellular areas of nonuniform Ca^{2+} decay were also recorded, however, within an oscillating cell (Fig. 10). Average whole-cell confocal fluorescence was plotted from two areas: a small subarea at the bottom of the cell (Fig. 10*A*, *dotted line*) and the rest of the cell (*solid line*). Steady caffeine application evoked an initial fluorescence increase that decayed to approximately baseline levels over most of the cell (*solid line*). Fluorescence in the subarea, however, decreased more slowly, held steady for ~1 sec, and then rose again during the second peak of the oscillation cycle. This persistent fluorescence again underscores the limited diffusibility of Ca^{2+} within these cells; whether the same Ca^{2+} ions remained steady in the subarea, or whether Ca^{2+} ions were being removed from and released into this area at the same rate, the elevated Ca^{2+} in the subarea did not diffuse into neighboring areas (Fig. 10*B*, *arrow*, compare *image series 2* and *3*). After the second peak in the oscillation cycle, fluorescence decayed within the subarea more slowly than in the rest of the cell, and a still smaller part of the marked subarea did not return to baseline levels. After each subsequent oscillation peak, fluorescence within the subarea returned fully to baseline in register with the rest of the cell, showing that the persistent fluorescence after the first two peaks was not caused by a locally high dye concentration.

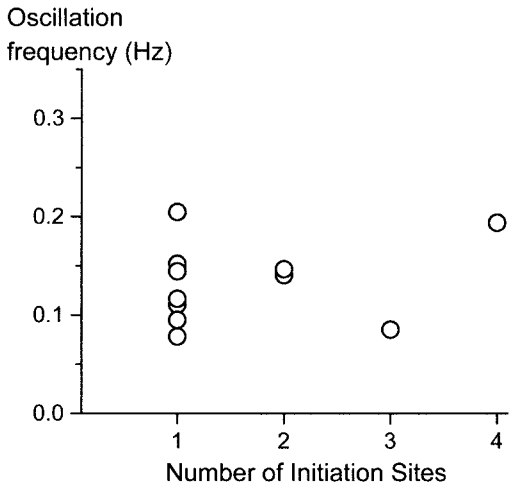

Figure 8. Oscillation frequency as a function of the number of oscillation initiation sites for each cell. Each point is from a separate cell. Because the oscillation frequency decreased gradually during a cycle, frequencies shown are approximate; frequency was calculated as the number of peaks in the oscillation cycle divided by the time from the onset of the first peak to the maximum of the last peak. A site was counted as an initiation site if fluorescence arising from that site triggered the spread of fluorescence for at least one peak within the oscillation cycle. For defining the number of initiation sites per cell, the first peak of the oscillation cycle was excluded because caffeine likely had not yet reached a uniform intracellular concentration. The three oscillating cells in which fluorescence increased without an obvious site of origin are not included in the graph; these cells oscillated with an average frequency of 0.27 Hz. No correlation was evident when oscillation frequency was calculated from only the first five oscillation peaks for each cell, instead of from the entire oscillation cycle.

The subarea of decreased uptake in this cell occurred at one of two functional release initiation sites. Release sites at 7 and 2 o'clock are visible in the first oscillation peak as areas of discrete fluorescence that arose independently of the wave front spreading from the left side of the cell (Fig. 10*B*, *image series 1*, *third* and *fifth frames*, *arrows*). This cell responded to continual caffeine application with an oscillation cycle of 12 peaks. After the first peak, 5 of the 11 subsequent peaks initiated from the 7 o'clock site, including the second and third peaks. The local area where Ca^{2+} did not decay fully after the first and second peaks in the oscillation cycle was also the site of initiation of the subsequent (second and third) peaks in the oscillation cycle, suggesting that continual release from Ca^{2+} stores contributed to the persistent local Ca^{2+} elevation. Again, this indicates that intracellular Ca^{2+} stores in different areas of the cell receiving the same stimulus need not necessarily act in concert.

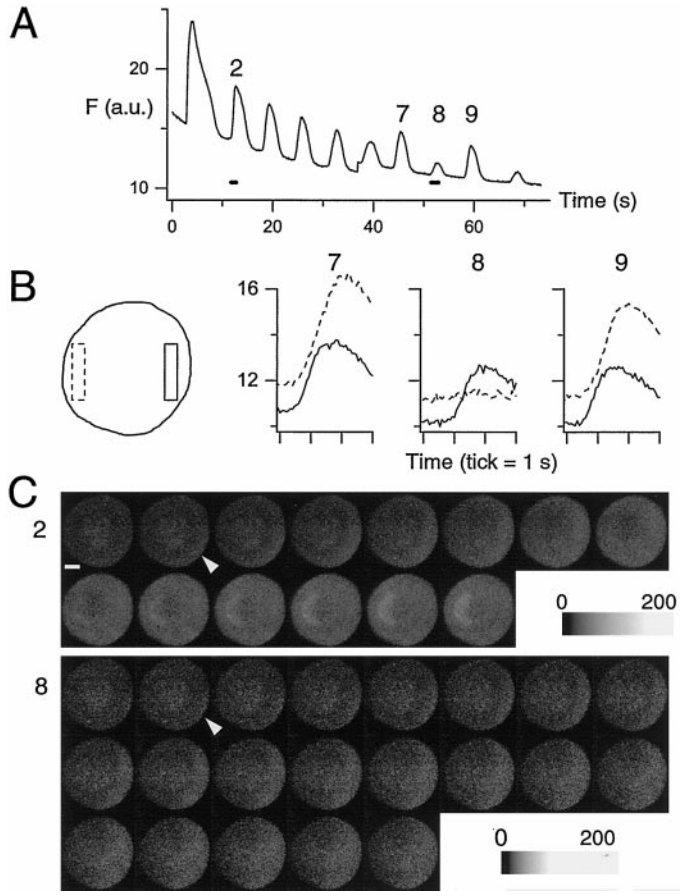

Figure 9. Failures of Ca^{2+} propagation. *A*, Time course of average fluorescence from within the entire cell in response to continual microperfusion of 10 mM caffeine. The jump in baseline fluorescence before the *sixth peak* in the oscillation cycle is attributable to the lowering of the neutral density filter (increased excitation intensity). The filter was also lowered at the upstroke of the *seventh peak*. *B*, Time course of average unsubtracted fluorescence within the subcellular areas enclosed by the *left* (*dotted line*) and *right* (*solid line*) *rectangles* during the *seventh*, *eighth*, and *ninth peaks* in the oscillation cycle. Background and peak fluorescence were slightly higher in the *left rectangle*. *C*, Consecutive images corresponding to the indicated intervals (*A*, *bars*) of *oscillation peaks 2* (*top*) and *8* (*bottom*). *Arrows* mark initiation sites of fluorescence for each oscillation peak. Scale bar, 10 μm. Because the *images* were faint, especially for *oscillation peak 8*, images were further scaled after background subtraction. Pixel values from 0 to 50 were linearly rebinned to fill the entire eight-bit 0–255 range, and the array was then smoothed. Color-coding for *image series 2* and *8* is marked by the *bar* at the end of each *image series*.

DISCUSSION

Data presented here indicate that, although Ca^{2+} release from intracellular stores took place throughout these neurons, discrete sites at the cell edge were preferentially primed to release Ca^{2+} throughout a cycle of Ca^{2+} oscillations. The corresponding patterns of Ca^{2+} release sites and of RyRs and SERCA pumps suggest a structural basis for the initiation and propagation of Ca^{2+}.

Discrete sites initiate Ca^{2+} release

The spatially smallest caffeine-evoked Ca^{2+} increases detected here, at the start of the Ca^{2+} wave fronts (compare Fig. 4), were a few micrometers wide, consistent with the size of elementary Ca^{2+} release events in other cells (Cheng et al., 1993; Bootman and Berridge, 1995; Tsugorka et al., 1995; Koizumi et al., 1999a; Lacampagne et al., 1999). We infer that Ca^{2+} wave fronts that were recorded here began by release through RyRs, analogous to a spark, that was then amplified via CICR.

Local Ca^{2+} signaling has not been obvious in imaging of Ca^{2+} oscillations in other neurons. In developing cortical (Flint et al., 1999) and cerebellar granule (Komuro and Rakic, 1996) neurons, the Ca^{2+} rise was uniform or somewhat larger in the cell center than at the edges. The simultaneous rise of Ca^{2+} over the entire cell body was also seen in pioneering studies in frog sympathetic neurons of Ca^{2+} oscillations evoked by depolarization plus caffeine (Lipscombe et al., 1988a). These oscillations occur at ~10-fold lower frequency than oscillations evoked by caffeine alone (Lipscombe et al., 1988a; Friel and Tsien, 1992b), so the mechanism of initial release could easily be different from that studied here. Uniform Ca^{2+} release across the cell body might reflect the presence or absence of organellar structures or the lack of variation in Ca^{2+} or caffeine sensitivity among RyRs. Confocal recordings from other neuronal types should indicate whether release from subareas at the cell edge is a more general mechanism for initiation of Ca^{2+} wave fronts in neurons.

How did release always initiate from the cell periphery, even with the uniform intracellular caffeine concentration (Fig. 2) present during oscillations? Staining experiments (Fig. 5) suggest that only at the cell periphery is the density of RyRs high enough for release of sufficient Ca^{2+} to activate neighboring RyRs and initiate a regenerative Ca^{2+} wave front. Bullfrog sympathetic neurons have high levels of caffeine-sensitive Ca^{2+} stores close to the plasma membrane within sub-surface cisterns (SSCs) of the ER network

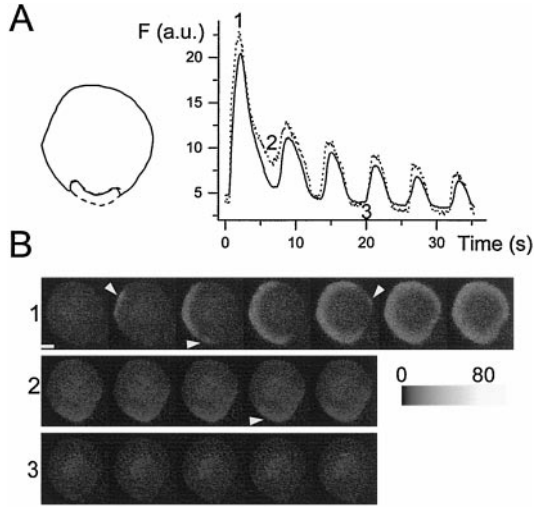

Figure 10. Locally elevated Ca^{2+} levels during interpeak periods of an oscillation cycle. *A*, Average pixel fluorescence within areas of the cell indicated by *solid* and *dotted lines* (*left*) is plotted as a function of time (*right*) in response to continual application of 10 mM caffeine. The *dotted line* corresponds to the fluorescence of the subarea; the *solid line* corresponds to the fluorescence of the rest of the cell. The first 6 of 12 oscillation peaks are displayed. The time course was made from background-subtracted images. *Numbered points* indicate the times of the corresponding confocal image series in *B*. *B*, Consecutive images recorded from the three points in the time course marked with the corresponding number—onset of the first oscillation peak (1), and the *troughs* between the first and second peaks (2), and third and fourth peaks (3). Pixel values from 0 to 80 for each image series are grayscale-coded according to the *look-up bar* after *image series 2*. *Image series 2* and *3* are smoothed; *image series 1* is not smoothed. *Arrows* in *series 1* at 10, 7, and 2 o'clock mark points at which fluorescence rose without a wave first propagating to the site. *Arrow* in *image series 2* indicates a persistent area of locally high fluorescence. Scale bar, 10 μm.

(Fujimoto et al., 1980). The discrete spots of high SERCA pump density at the cell periphery (Fig. 6) suggest a possible mechanism for the formation of these high $[Ca^{2+}]$ deposits, although we do not know whether the SERCA pump hot spots correspond to SSCs. Clearly, however, these neurons have distinct sites, just under the plasma membrane, of preferential release of Ca^{2+}, of high SERCA pump density, and of high Ca^{2+} storage levels (Fujimoto et al., 1980). This implies functional specialization of different regions apposed to the plasma membrane. It is tempting to speculate that caffeine-evoked intracellular Ca^{2+} release is initiated via RyRs from SSCs directly underneath the cell membrane that have been filled with Ca^{2+} by locally high levels of SERCA pumps. Many types of neurons have SSCs (Rosenbluth, 1962; Watanabe and Burnstock, 1976; Henkart et al., 1978; Berridge, 1998) or clusters of RyRs or $InsP_3$Rs similar to these neurons. In cerebellar neurons, for example, a high density of $InsP_3$Rs is found in the membranes of ER cisternal stacks (Satoh et al., 1990; Takei et al., 1992), and junctions analogous to the muscle triad have been viewed between cisternal and plasma membranes in several types of neuron (Henkart et al., 1976, Henkart, 1980). Ca^{2+} release channels seem to be commonly apposed to subareas of the ER; further work is required to show functional roles for these subareas during Ca^{2+} release or oscillations.

If RyRs at the release initiation sites recorded here were indeed apposed to higher lumenal Ca^{2+} levels than others, these RyRs might be gated by lower levels of cytoplasmic Ca^{2+}, analogous to RyRs in bilayers and PC12 cells (Gyorke and Gyorke, 1998; Koizumi et al., 1999b), and thereby initiate the Ca^{2+} wave front. Some evidence for differences in sensitivity among RyRs to caffeine (and to Ca^{2+}) (Rousseau et al., 1988; Sitsapesan and Williams, 1990) in these neurons is found in the location of the initial Ca^{2+} rise. On the first caffeine application, RyRs on the right side of the cell responded first in a few cells (5 of 47; Table 1), even though the right side of the cell had a lower caffeine concentration (Fig. 2). This suggests differences in caffeine sensitivity among different release sites; otherwise initial release would always have been from the left. Ca^{2+} stores with different agonist sensitivities have also been proposed for $InsP_3$-sensitive stores in nonexcitable cells (Parker and Yao, 1991; Kasai et al., 1993; Thorn et al., 1993; Bootman et al., 1994), and among RyRs in chromaffin cells (Cheek et al., 1994). Higher sensitivity to Ca^{2+} or caffeine, or greater capacity of RyRs in our cells, however, could itself be a by-product of modification of RyRs or other molecules by phosphorylation, calmodulin, cyclic ADP-ribose, or other Ca^{2+}-activated signaling pathways. The location of each Ca^{2+} release initiation site at the cell edge also suggests modification by molecules of the plasma membrane.

Propagation of the Ca^{2+} wave front

Based on the rise time of fluorescence in subareas at the cell periphery, Ca^{2+} release began and ended within 200 msec, faster than the wave front extended over the entire cell (Figs. 1*C*, 3*C*, 4*C*, 7*C*). However, based on the low Ca^{2+} diffusibility observed in many cells (Figs. 3, 9, 10), passive Ca^{2+} spread in these neurons appears to be quite low. This suggests that Ca^{2+} wave front propagation in these neurons is best viewed as a sequential series of fast Ca^{2+} release events at neighboring sites. Higher RyR density at the cell periphery may account for faster circumferential than radial propagation. Although the CICR mechanism itself requires microdiffusion of Ca^{2+} for release from one RyR site to activate release at adjacent RyRs, elevated Ca^{2+} levels that were not part of a propagating wave front (Figs. 9, 10) appeared effectively immobile. Because, in most cases, and always on initial caffeine application, Ca^{2+} propagated without obvious discontinuity, the RyRs that form Ca^{2+} release sites may form an almost continuous distribution. Because Ca^{2+} wave fronts initiate at the same site (or sites) for each peak in an oscillation cycle, propagation failures could result in consistent activation of Ca^{2+} signaling pathways in only certain subcellular areas.

Physiological implications

In other cell types, locally nonuniform Ca^{2+} levels during $InsP_3$-dependent Ca^{2+} oscillations may contribute to exocytosis and fluid secretion or reflect the sites of hormonal stimulation (Kasai and Augustine, 1990; Rooney et al., 1990; Nathanson et al., 1992; Toescu et al., 1992; Hille et al., 1994; Tse et al., 1997). What might be a corresponding functional role for the patterns of Ca^{2+} release via RyRs described here? Frog neurons receive synapses on the cell body (Adams et al., 1986); a release initiation site adjacent to the plasma membrane is ideally situated to amplify Ca^{2+} influx through the plasma membrane into a propagating Ca^{2+} wave front. Such amplification would turn a local Ca^{2+} increase into a Ca^{2+} increase as far as the Ca^{2+} wave front propagated. We further speculate that modulation of Ca^{2+} influx across the plasma membrane, or of RyR Ca^{2+} sensitivity, at just the release initiation site could be a method for local modulation to affect cell-wide Ca^{2+} levels. Although Ca^{2+} influx without additional RyR agonists induces CICR in these and other neurons (Friel and Tsien, 1992a; Hua et al., 1993, 1994; Llano et al., 1994; Shmigol et al., 1995; Peng, 1996; Usachev and Thayer, 1997) (but see Cohen et al., 1997), CICR is more likely when RyRs have been sensitized to cytoplasmic Ca^{2+}. A physiological analog of caffeine is not firmly established, although increased levels of cyclic ADP-ribose or activity of kinases or calmodulin have been proposed to play this role (Hua et al., 1994; Lee et al., 1994). Weakening of cytoplasmic Ca^{2+} buffering might be even more effective than sensitization of the RyRs for triggering CICR. In several cell types, only ~1% of cytoplasmic Ca^{2+} is free (Hille et al., 1994); even a modest decrease in cytoplasmic buffering efficacy could dramatically increase the free Ca^{2+} available to initiate CICR.

In conclusion, high-speed imaging has revealed a potential organellar basis for subcellular Ca^{2+} signaling and Ca^{2+} wave front propagation in these neurons. It will be interesting to see whether similar mechanisms initiate or mediate Ca^{2+} oscillations during neuronal migration or other physiological processes.

REFERENCES

Adams PR, Jones SW, Pennefather P, Brown DA, Koch C, Lancaster B (1986) Slow synaptic transmission in frog sympathetic ganglia. J Exp Biol 124:259–285.

Berridge MJ (1998) Neuronal calcium signaling. Neuron 21:13–26.

Bootman MD, Berridge MJ (1995) The elemental principles of calcium signaling. Cell 83:675–678.

Bootman MD, Cheek TR, Moreton RB, Bennett DL, Berridge MJ (1994) Smoothly graded Ca^{2+} release from inositol 1,4,5-trisphosphate-sensitive Ca^{2+} stores. J Biol Chem 269:24783–24791.

Cheek TR, Berridge MJ, Moreton RB, Stauderman KA, Murawsky MM, Bootman MD (1994) Quantal Ca^{2+} mobilization by ryanodine receptors is due to all-or-none release from functionally discrete intracellular stores. Biochem J 301:879–883.

Cheng H, Lederer WJ, Cannell MB (1993) Calcium sparks: elementary events underlying excitation–contraction coupling in heart muscle. Science 262:740–744.

Clapham DE (1995) Calcium signaling. Cell 80:259–268.

Cohen AS, Moore KA, Bangalore R, Jafri MS, Weinreich D, Kao JP (1997) Ca^{2+}-induced Ca^{2+} release mediates Ca^{2+} transients evoked by single action potentials in rabbit vagal afferent neurones. J Physiol (Lond) 499:315–328.

Cseresnyés Z, Bustamante AI, Klein MG, Schneider MF (1997) Release-activated Ca^{2+} transport in neurons of frog sympathetic ganglia. Neuron 19:403–419.

Cseresnyés Z, Bustamante AI, Schneider MF (1999) Caffeine-induced $[Ca^{2+}]$ oscillations in neurones of frog sympathetic ganglia. J Physiol (Lond) 514:83–99.

De Koninck P, Schulman H (1998) Sensitivity of CaM kinase II to the frequency of Ca^{2+} oscillations. Science 279:227–230.

Dolmetsch RE, Xu K, Lewis RS (1998) Calcium oscillations increase the efficiency and specificity of gene expression. Nature 392:933–936.

Empson RM, Galione A (1997) Cyclic ADP-ribose enhances coupling between voltage-gated Ca^{2+} entry and intracellular Ca^{2+} release. J Biol Chem 272:20967–20970.

Escobar AL, Velez P, Kim AM, Cifuentes F, Fill M, Vergara JL (1997) Kinetic properties of DM-nitrophen and calcium indicators: rapid transient response to flash photolysis. Pflügers Arch 434:615–631.

Fewtrell C (1993) Ca^{2+} oscillations in non-excitable cells. Annu Rev Physiol 55:427–454.

Finch EA, Augustine GJ (1998) Local calcium signalling by inositol-1,4,5-trisphosphate in Purkinje cell dendrites. Nature 396:753–756.

Flint AC, Dammerman RS, Kriegstein AR (1999) Endogenous activation of metabotropic glutamate receptors in neocortical development causes neuronal calcium oscillations. Proc Natl Acad Sci USA 96:12144–12149.

Friel DD (1995) $[Ca^{2+}]_i$ oscillations in sympathetic neurons: an experimental test of a theoretical model. Biophys J 68:1752–1766.

Friel DD, Tsien RW (1992a) A caffeine- and ryanodine-sensitive Ca^{2+} store in bullfrog sympathetic neurones modulates effects of Ca^{2+} entry on $[Ca^{2+}]_i$. J Physiol (Lond) 450:217–246.

Friel DD, Tsien RW (1992b) Phase-dependent contributions from Ca^{2+} entry and Ca^{2+} release to caffeine-induced $[Ca^{2+}]$ oscillations in bullfrog sympathetic neurons. Neuron 8:1109–1125.

Friel DD, Tsien RW (1994) An FCCP-sensitive Ca^{2+} store in bullfrog sympathetic neurons and its participation in stimulus-evoked changes in $[Ca^{2+}]_i$. J Neurosci 14:4007–4024.

Fujimoto S, Yamamoto K, Kuba K, Morita K, Kato E (1980) Calcium localization in the sympathetic ganglion of the bullfrog and effects of caffeine. Brain Res 202:21–32.

Ghosh A, Greenberg ME (1995) Calcium signaling in neurons: molecular mechanisms and cellular consequences. Science 268:239–247.

Golovina VA, Blaustein MP (1997) Spatially and functionally distinct Ca^{2+} stores in sarcoplasmic and endoplasmic reticulum. Science 275:1643–1648.

Gomez TM, Spitzer NC (1999) In vivo regulation of axon extension and pathfinding by growth-cone calcium transients. Nature 397:350–355.

Gu X, Spitzer NC (1995) Distinct aspects of neuronal differentiation encoded by frequency of spontaneous Ca^{2+} transients. Nature 375:784–787.

Gyorke I, Gyorke S (1998) Regulation of the cardiac ryanodine receptor channel by luminal Ca^{2+} involves luminal Ca^{2+} sensing sites. Biophys J 75:2801–2810.

Henkart M (1980) Identification and function of intracellular calcium stores in axons and cell bodies of neurons. Fed Proc 39:2783–2789.

Henkart M, Landis DMD, Reese TS (1976) Similarity of junctions between plasma membranes and endoplasmic reticulum in muscle and neurons. J Cell Biol 70:338–347.

Henkart MP, Reese TS, Brinley Jr FJ (1978) Endoplasmic reticulum sequesters calcium in the squid giant axon. Science 202:1300–1303.

Hernandez-Cruz A, Sala F, Adams PR (1990) Subcellular calcium transients visualized by confocal microscopy in a voltage-clamped vertebrate neuron. Science 247:858–862.

Hille B, Tse A, Tse FW, Almers W (1994) Calcium oscillations and exocytosis in pituitary gonadotrophs. Ann NY Acad Sci 710:261–270.

Hong K, Nishiyama M, Henley J, Tessier-Lavigne M, Poo M-M (2000) Calcium signaling in the guidance of nerve growth by netrin-1. Nature 403:93–98.

Hua SY, Nohmi M, Kuba K (1993) Characteristics of Ca^{2+} release induced by Ca^{2+} influx in cultured bullfrog sympathetic neurons. J Physiol (Lond) 464:245–272.

Hua SY, Tokimasa T, Takasawa S, Furuya Y, Nohmi M, Okamoto H, Kuba K (1994) Cyclic ADP-ribose modulates Ca^{2+} release channels for activation by physiological Ca^{2+} entry in bullfrog sympathetic neurons. Neuron 12:1073–1079.

Kasai H, Augustine GJ (1990) Cytosolic Ca^{2+} gradients triggering unidirectional fluid secretion from exocrine pancreas. Nature 348:735–738.

Kasai H, Li YX, Miyashita Y (1993) Subcellular distribution of Ca^{2+} release channels underlying Ca^{2+} waves and oscillations in exocrine pancreas. Cell 74:669–677.

Kennedy MB (1989) Regulation of neuronal function by calcium. Trends Neurosci 12:417–420.

Kirkwood A, Simmons MA, Mather RJ, Lisman J (1991) Muscarinic suppression of the M-current is mediated by a rise in internal Ca^{2+} concentration. Neuron 6:1009–1014.

Koizumi S, Bootman MD, Bobanovic LK, Schell MJ, Berridge MJ, Lipp P (1999a) Characterization of elementary Ca^{2+} release signals in NGF-differentiated PC12 cells and hippocampal neurons. Neuron 22:125–137.

Koizumi S, Lipp P, Berridge MJ, Bootman MD (1999b) Regulation of ryanodine receptor opening by lumenal Ca^{2+} underlies quantal Ca^{2+} release in PC12 cells. J Biol Chem 274:33327–33333.

Komuro H, Rakic P (1996) Intracellular Ca^{2+} fluctuations modulate the rate of neuronal migration. Neuron 17:275–285.

Kuba K, Nishi S (1976) Rhythmic hyperpolarizations and depolarization of sympathetic ganglion cells induced by caffeine. J Neurophysiol 39:547–563.

Lacampagne A, Ward CW, Klein MG, Schneider MF (1999) Time course of individual Ca^{2+} sparks in frog skeletal muscle recorded at high time resolution. J Gen Physiol 113:187–198.

Lattanzio Jr FA, Bartschat DK (1991) The effect of pH on rate constants, ion selectivity, and thermodynamic properties of fluorescent calcium and magnesium indicators. Biochem Biophys Res Commun 177:184–191.

Lee HC, Aarhus R, Graeff R, Gurnack ME, Walseth TF (1994) Cyclic ADP ribose activation of the ryanodine receptor is mediated by calmodulin. Nature 370:307–309.

Li W, Llopis J, Whitney M, Zlokarnik G, Tsien RY (1998) Cell-permeant caged $InsP_3$ ester shows that Ca^{2+} spike frequency can optimize gene expression. Nature 392:936–941.

Lipscombe D, Madison DV, Poenie M, Reuter H, Tsien RW, Tsien RY (1988a) Imaging of cytosolic Ca^{2+} transients arising from Ca^{2+} stores and Ca^{2+} channels in sympathetic neurons. Neuron 1:355–365.

Lipscombe D, Madison DV, Poenie M, Reuter H, Tsien RY, Tsien RW (1988b) Spatial distribution of calcium channels and cytosolic calcium transients in growth cones and cell bodies of sympathetic neurons. Proc Natl Acad Sci USA 85:2398–2402.

Llano I, DiPolo R, Marty A (1994) Calcium-induced calcium release in cerebellar Purkinje cells. Neuron 12:663–673.

Lukyanenko V, Subramanian S, Gyorke E, Wiesner TF, Gyorke S (1999) The role of luminal Ca^{2+} in the generation of Ca^{2+} waves in rat ventricular myocytes. J Physiol (Lond) 518:173–186.

Maeda H, Ellis-Davies GCR, Ito K, Miyashita Y, Kasai H (1999) Supralinear Ca^{2+} signaling by cooperative and mobile Ca^{2+} buffering in Purkinje neurons. Neuron 24:989–1002.

McPherson PS, Kim Y-K, Valdivia H, Knudson CM, Takekura H, Franzini-Armstrong C, Coronado R, Campbell KP (1991) The brain ryanodine receptor: caffeine-sensitive calcium release channel. Neuron 7:17–25.

Meldolesi J, Pozzan T (1998) The heterogeneity of ER Ca^{2+} stores has a key role in nonmuscle cell signaling and function. J Cell Biol 142:1395–1398.

Minta A, Kao JPY, Tsien RY (1989) Fluorescent indicators for cytosolic calcium based on rhodamine and fluorescein chromophores. J Biol Chem 264:8171–8178.

Muschol M, Dasgupta BR, Salzberg BM (1999) Caffeine interaction with fluorescent calcium indicator dyes. Biophys J 77:577–586.

Nasi E, Tillotson D (1985) The rate of diffusion of Ca^{2+} and Ba^{2+} in a nerve cell body. Biophys J 47:735–738.

Nathanson MH, Padfield PJ, O'Sullivan AJ, Burgsthaler AD, Jamieson JD (1992) Mechanism of Ca^{2+} wave propagation in pancreatic acinar cells. J Biol Chem 267:18118–18121.

Neering IR, McBurney RN (1984) Role for microsomal Ca storage in mammalian neurons? Nature 309:158–160.

Parker I, Yao Y (1991) Regenerative release of calcium from functionally discrete subcellular stores by inositol trisphosphate. Proc R Soc Lond B Biol Sci 246:269–274.

Peng Y (1996) Ryanodine-sensitive component of calcium transients evoked by nerve firing at presynaptic nerve terminals. J Neurosci 16:6703–6712.

Perez-Terzic C, Stehno-Bittel L, Clapham DE (1997) Nucleoplasmic and cytoplasmic differences in the fluorescence properties of the calcium indicator Fluo-3. Cell Calcium 21:275–282.

Pfaffinger PJ, Leibowitz MD, Subers EM, Nathanson NM, Almers W, Hille B (1988) Agonists that suppress M-current elicit phosphoinositide turnover and Ca^{2+} transients, but these events do not explain M-current suppression. Neuron 1:477–484.

Pivovarova NB, Hongpaisan J, Andrews SB, Friel DD (1999) Depolarization-induced mitochondrial Ca accumulation in sympathetic neurons: spatial and temporal characteristics. J Neurosci 19:6372–6384.
Pozzan T, Rizzuto R, Volpe P, Meldolesi J (1994) Molecular and cellular physiology of intracellular calcium stores. Physiol Rev 74:595–636.
Rooney TA, Sass EJ, Thomas AP (1990) Agonist-induced cytosolic calcium oscillations originate from a specific locus in single hepatocytes. J Biol Chem 265:10792–10796.
Rosenbluth J (1962) Subsurface cisterns and their relationship to the neuronal plasma membrane. J Cell Biol 13:405–421.
Rousseau E, LaDine J, Liu Q-Y, Meissner G (1988) Activation of the Ca^{2+} release channel of skeletal muscle sarcoplasmic reticulum by caffeine and related compounds. Arch Biochem Biophys 267:75–86.
Satoh T, Ross CA, Villa A, Supattapone S, Pozzan T, Snyder SH, Meldolesi J (1990) The inositol 1,4,5,-trisphosphate receptor in cerebellar Purkinje cells: quantitative immunogold labeling reveals concentration in an ER subcompartment. J Cell Biol 111:615–624.
Shmigol A, Verkhratsky A, Isenberg G (1995) Calcium-induced calcium release in rat sensory neurons. J Physiol (Lond) 489:627–636.
Sitsapesan R, Williams AJ (1990) Mechanisms of caffeine activation of single calcium-release channels of sheep cardiac sarcoplasmic reticulum. J Physiol (Lond) 423:425–439.
Smith SJ, MacDermott AB, Weight FF (1983) Detection of intracellular Ca^{2+} transients in sympathetic neurones using arsenazo III. Nature 304:350–352.
Takechi E, Eilers J, Konnerth A (1998) A new class of synaptic response involving calcium release in dendritic spines. Nature 396:757–760.
Takei K, Stukenbrok H, Metcalf A, Mignery GA, Sudhof TC, Volpe P, De Camilli P (1992) Ca^{2+} stores in Purkinje neurons: endoplasmic reticulum subcompartments demonstarated by the heterogeneous distribution of the $InsP_3$ receptor, Ca^{2+}-ATPase, and calsequestrin. J Neurosci 12:489–505.
Tepikin AV, Petersen OH (1992) Mechanisms of cellular calcium oscillations in secretory cells. Biochim Biophys Acta 1137:197–207.
Thayer SA, Hirning LD, Miller RJ (1988) The role of caffeine-sensitive calcium stores in the regulation of free intracellular calcium in rat sympathetic neurons in vitro. Mol Pharmacol 34:664–673.
Thomas AP, Bird GSJ, Hajnoczky G, Robb-Gaspers LD, Putney Jr JW (1996) Spatial and temporal aspects of cellular calcium signaling. FASEB J 10:1505–1517.
Thorn P, Lawrie AM, Smith PM, Gallacher DV, Petersen OH (1993) Local and global cytosolic Ca^{2+} oscillations in exocrine cells evoked by agonists and inositol trisphosphate. Cell 74:661–668.
Toescu EC, Lawrie AM, Petersen OH, Gallacher DV (1992) Spatial and temporal distribution of agonist-evoked cytoplasmic Ca^{2+} signals in exocrine acinar cells analysed by digital image microscopy. EMBO J 11:1623–1629.
Tse FW, Tse A, Hille B, Horstmann H, Almers W (1997) Local Ca^{2+} release from internal stores controls exocytosis in pituitary gonadotrophs. Neuron 18:121–132.
Tsien RW, Tsien RY (1990) Calcium channels, stores, and oscillations. Annu Rev Cell Biol 6:715–760.
Tsien RY, Bacskai BJ (1995) Video-rate confocal microscopy. In: Handbook of biological confocal microscopy (Pawley JB, ed), pp 459–478. New York: Plenum.
Tsugorka A, Rios E, Blatter LA (1995) Imaging elementary events of calcium release in skeletal muscle cells. Science 269:1723–1726.
Usachev YM, Thayer SA (1997) All-or-none release Ca^{2+} from intracellular stores triggered by Ca^{2+} influx through voltage-gated Ca^{2+} channels in rat sensory neurons. J Neurosci 17:7404–7414.
Watanabe H, Burnstock G (1976) Junctional subsurface organs in frog sympathetic ganglion cells. J Neurocytol 5:125–136.
Zheng JQ (2000) Turning of growth cones induced by localized increases in intracellular calcium ions. Nature 403:89–93.